

Study of the conditions for the effective energy transfer in a process of acceleration and collision of the thin metal disks with the massive target

S. Borodziuk¹, A. Kasperczuk¹, T. Pisarczyk^{1,a}, S.Yu. Gus'kov², J. Ullschmied³, E. Krousky⁴, K. Masek⁴, M. Pfeifer⁴, K. Rohlena⁴, J. Skala⁴, M. Kalal⁵, J. Limpouch⁵, and P. Pisarczyk⁶

¹ Institute of Plasma Physics and Laser Microfusion, 23 Hery St., 00-908 Warsaw, Poland

² P.N. Lebedev Physical Institute of RAS, 53 Leninsky Ave., 119 991 Moscow, Russia

³ Institute of Plasma Physics AS CR, Za Slovankou 3, 182 00 Prague 8, Czech Republic

⁴ Institute of Physics AS CR, Na Slovance 2, 182 21 Prague 8, Czech Republic

⁵ Czech Technical University in Prague, FNSPE, Brehova 7, 115 19 Prague 1, Czech Republic

⁶ Warsaw University of Technology, ICS, 15/19 Nowowiejska St., 00-665 Warsaw, Poland

Received 5 April 2006 / Received in final form 31 May 2006

Published online 6 October 2006 – © EDP Sciences, Società Italiana di Fisica, Springer-Verlag 2006

Abstract. Efficiency studies of laser driven thin metal disks acceleration using the first harmonic ($\lambda_1 = 1.315 \mu\text{m}$) of the Prague Asterix Laser System (PALS) and subsequent craters creation produced by collisions of these disks with massive targets are presented. Several different disks made of aluminium and copper foils with diameters of $300 \mu\text{m}$ and $600 \mu\text{m}$ and thicknesses of $11 \mu\text{m}$ (Al) and $3.6 \mu\text{m}$ (Cu) were employed. Disks were placed at the distance of either $100 \mu\text{m}$ or $300 \mu\text{m}$ in front of aluminium massive targets. The following irradiation conditions were used: the laser beam energy of 120 J, the focal spot diameter of $200 \mu\text{m}$, and the pulse duration of 0.4 ns (FWHM). A three-frame interferometric system was employed to determine electron density distributions in plasma corona. Shape and volume of craters were obtained by crater replica technology and microscopy measurements. The aim of these investigations was to analyse conditions leading to the most effective energy transfer in the process of collision of the accelerated disks with solid targets. The overall efficiency of these processes was characterized by the volume of craters produced in such targets.

PACS. 52.38.Mf Laser ablation – 52.50.Jm Plasma production and heating by laser beams (laser-foil, laser-cluster, etc.) – 79.20.Ds Laser-beam impact phenomena

1 Introduction

It is a well established fact that high power lasers can be used to efficiently accelerate thin targets (flyers) to very high velocities — reaching 10^7 cm/s and more. During the subsequent collision of the accelerated flyer with a massive target the flyer's kinetic energy is rapidly transferred into a massive target in the form of thermal energy. It leads to generation of an extremely high pressure in a planar shock. Consequently, this process is a subject of great interest for important areas of modern physics, such as determination of the equation of state (EOS) in materials under extreme conditions, modifications of physical properties of materials, etc. [1–7]. The flyer-impact configuration could also play an important role in the field of inertial confinement fusion. Recently the so-called impact fast ignition was proposed [8,9], where the flyer impact en-

ergy is used to ignite a relatively cold fuel precompressed by the main laser driver.

Investigations of planar shocks can be realized by the following two different approaches:

- *a dynamical method*, which is based on streak-camera measurements of the actual shock velocity in thin foils made of different materials. These investigations, being performed by many scientific groups for last twenty years or longer, are mainly devoted to determination of the equation of state of different materials in high pressure conditions (e.g. [2,6,7]);
- *a static method*, for which the essential information is obtained from the crater created directly or indirectly in solid targets. Crater parameters, such as volume, shape, dimensions and symmetry, connected with interferometric measurements of a plasma corona (e.g. plasma dynamics, plasma torch dimensions, electron density distribution and total number of electrons) are very important data for subsequent theoretical

^a e-mail: pisaro@ifpilm.waw.pl

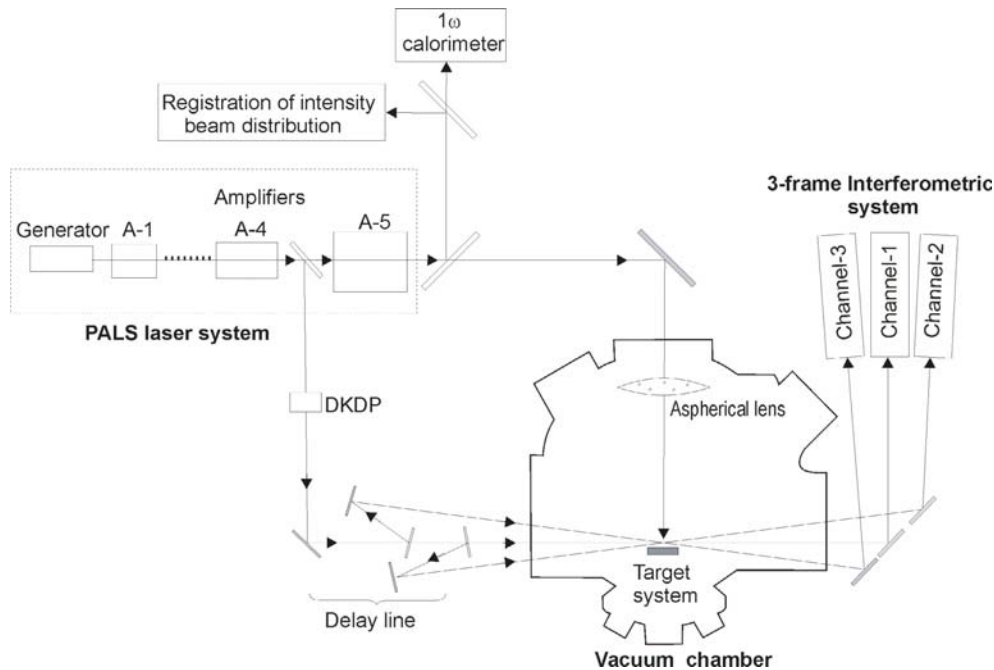


Fig. 1. Experimental set-up.

analyses by means of the 2-D theoretical model prepared by the theoretical group from the Lebedev Institute in Moscow [10,11] and developed by Gus'kov [12]. This, relatively simple, method allows to obtain substantial information about all the processes connected with the laser beam-target interaction, starting from the laser energy absorption, and finishing with the creation of craters. This information could be obtained only by using the static (integrated) method. Because the experimental and theoretical results of the direct laser action on massive target, presented in [12], turned out to be very interesting it was our intention using the above mentioned model for analyses of indirect laser action by means of thin foil or disk.

Our earlier investigations of the flyers [13–16] were concentrated on determination of macroparticles acceleration and craters creation efficiency with respect to: (i) the macroparticle type (the extracted foil fragment or prefabricated disk) and (ii) the laser beam wavelength (the first or third harmonic of the iodine laser). Attention was also paid to the delay in the flyer's getting under way with respect to the laser pulse timing, final velocity achieved for different target thickness and wavelength employed.

In the experiment described in this paper the flyers were all in the form of prefabricated disks only. The main attention was focused on determination of the influence of some other parameters on the efficiency of craters production, namely the disk diameter, the disk distance from the massive target and the disk material.

There were two reasons for which optimization of the above mentioned disk parameters seemed to be of importance:

- relatively a low efficiency of the crater creation by the disk with the diameter only a bit greater than the fo-

cal spot one compared to the crater creation efficiency related to the direct laser beam action itself;

- a strong influence of the disk holder type (thin mylar foil vs. carbon fibres) on the crater creation efficiency (the crater volume was about three times larger in the foil holder case — mainly due to noticeably bigger crater diameter).

Explanation of these unexpected problems was indispensable for our further theoretical analyses.

To study the temporal and spatial behaviours of the plasma expansion in experiments performed a three-frame interferometric system was used. Additionally, the crater replica technology and optical microscopy were employed to determine the crater profiles and dimensions.

2 Experimental set-up

The experimental investigations were carried out on the PALS iodine laser facility [17]. Its optical scheme is depicted in Figure 1.

The laser provided a 0.4 ns (FWHM) pulse with the energy of 120 J at the first harmonic ($\lambda_1 = 1.315 \mu\text{m}$). The full laser beam diameter at the target chamber entrance window was about 290 mm. Inside the chamber it was focused by means of an aspherical lens with a focal length of 627 mm reaching the focal spot diameter of $200 \mu\text{m}$ on the target (the focal point was located inside the target). In this case the laser intensity on the target surface was $0.95 \times 10^{15} \text{ W/cm}^2$. Intensity distributions across the laser beam cross-section were recorded in each laser shot by the CCD camera. They clearly proved a very high homogeneity of the intensity distribution across the

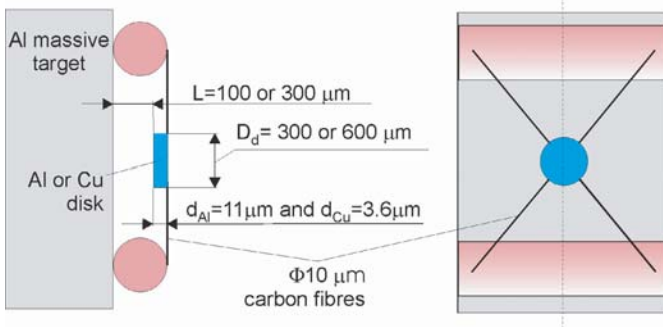


Fig. 2. Construction of the double targets.

whole cross-section of the laser beam. To avoid diffraction effects, which could disturb the laser beam intensity distribution on the target surface, retransmission of the beam on the target through the soft diaphragm placed in the laser system, as well as a proper space beam filtration were used.

Several different combinations of thin metal disks placed in front of massive targets were employed. The construction of such double-targets used in these experiments is shown in Figure 2. The massive part of the double-targets was always made of aluminium. The disks were made of either Al or Cu and their diameters were set to $300 \mu\text{m}$ or $600 \mu\text{m}$. Their thicknesses were chosen as $3.6 \mu\text{m}$ in the case of the Cu and $11 \mu\text{m}$ in the case of the Al. The selected Cu disk thickness was comparable to the Al disk one in the sense of the surface density

($\rho_{\text{Cu}}d_{\text{Cu}} = \rho_{\text{Al}}d_{\text{Al}}$, where: ρ is the mass density of the disk material and d is its thickness). Two different gaps separating the disk and the massive targets ($100 \mu\text{m}$ and $300 \mu\text{m}$) were employed.

To study the plasma expansion and flyer disk acceleration, a 3-frame interferometric system with automatic image processing was employed. Each of the interferometric channels was equipped with its own independent interferometer of the folding wave type. The diagnostic beam was obtained as a part of the main laser beam subsequently converted to the third harmonic. The delay between the frames was 3 ns.

In order to obtain information about the shape and dimensions of the craters, their replicas were made of cellulose acetate. To reconstruct qualitatively the crater shape, profiles of the crater replica in chosen cross-sections were digitized and the data used for calculations.

3 Experimental results

3.1 Results of interferometric measurements

In this section some typical results of our interferometric measurements will be presented. In Figure 3 two sequences of electron density distributions corresponding to three different instants of figures are related to the moment of the laser action). These data were obtained for the Al disks with the diameters of $300 \mu\text{m}$ and $600 \mu\text{m}$ placed at the distance of $L = 300 \mu\text{m}$ from the massive

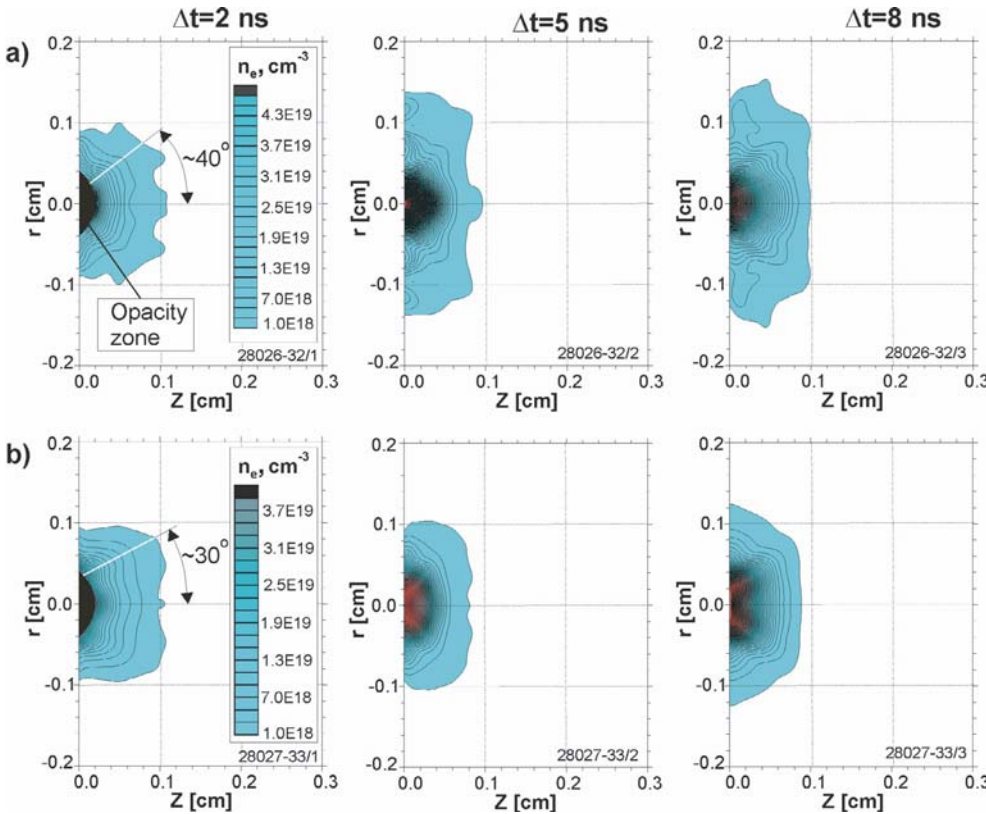


Fig. 3. Sequences of the electron densitograms correspond to two Al disk diameters: (a) $D_d = 300 \mu\text{m}$ and (b) $D_d = 600 \mu\text{m}$. On the first frames the maximum angle of plasma expansion is marked.

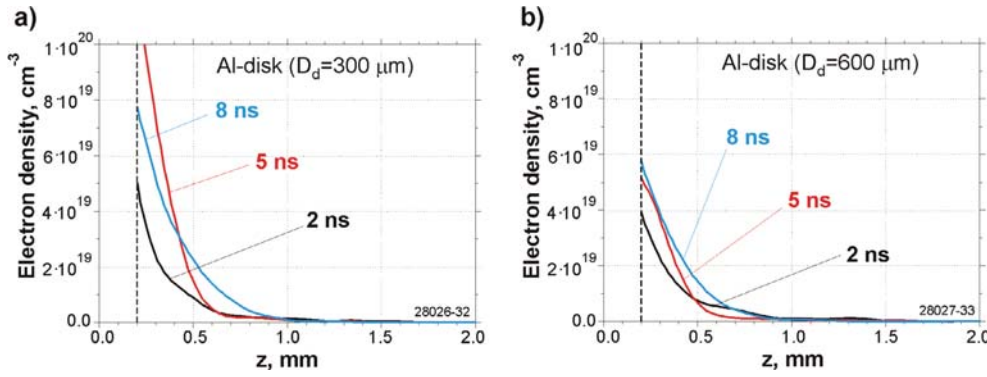


Fig. 4. Electron density distributions along the axis “ z ” for Al disks with the separation distance of $300 \mu\text{m}$ and different disk diameters: (a) $D_d = 300 \mu\text{m}$ and (b) $D_d = 600 \mu\text{m}$.

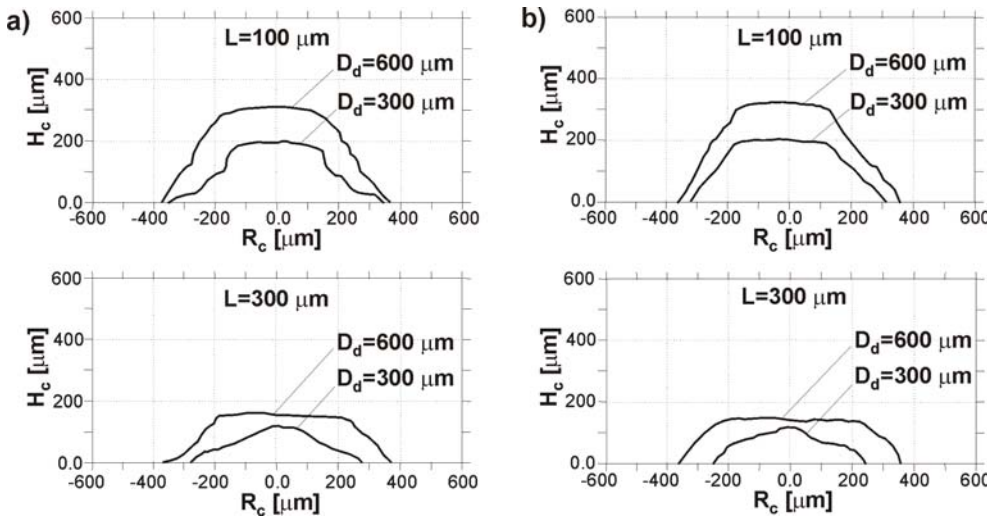


Fig. 5. Craters shapes and dimensions for: (a) Al disks and (b) Cu disks, where: R_c – crater radius and H_c – crater depth.

target. Here the plasma stream boundary is represented by the electron density contour of $n_e = 10^{18} \text{ cm}^{-3}$. All subsequent equidensity lines are always separated by the value of $2 \times 10^{18} \text{ cm}^{-3}$. The presented electron density distributions always start from the initial disk surface position, denoted here as $z = 0$.

The cases of disks with diameters of $300 \mu\text{m}$ and $600 \mu\text{m}$ exhibit considerable differences in the form of their corresponding plasma formation. One of them is characterized by the maximum angle of the main plasma stream outflow which is clearly different in both cases. This angle amounts to about 40° and 30° for the case of the $300 \mu\text{m}$ and $600 \mu\text{m}$ diameter disk, respectively. The smaller diameter disk exhibits the higher divergence of the plasma stream. The other difference is apparent in Figure 4, where corresponding electron densities measured along the z -axis are presented for the same types of disks as above. These densities representing the plasma corona are noticeably higher in the case of the smaller disk during the whole observation period, despite the higher plasma divergence.

3.2 Characteristics of craters

The crater profiles corresponding to all cases under consideration are presented in Figure 5. The following important

conclusions can be drawn from them:

- there is no substantial difference between the crater shapes related to Al and Cu disk materials provided that their diameters and masses (thus the surface mass densities as well) are the same;
- most of the craters have a trapezoidal shape, except the craters produced by the $300 \mu\text{m}$ diameter disk while using the gap of $300 \mu\text{m}$; in this particular case the crater shapes are exhibiting rather the conical form;
- the craters produced by the disks with smaller diameter are much shallower, whereas their diameters are only a bit smaller than those produced by the greater diameter disks.

Dependences of the crater volumes (averaged over several shots) on the gap employed for the both target materials are presented in Figure 6. The crater volume clearly decreases with the increasing gap. The ratio of the average crater volumes at $L = 100 \mu\text{m}$ and $L = 300 \mu\text{m}$ in all cases under consideration is equal to about 2.1.

In our opinion, to compare the crater volumes produced by the disks made of different materials the surface mass densities of the disks should be the same. Because in our experiment this requirement was not exactly satisfied

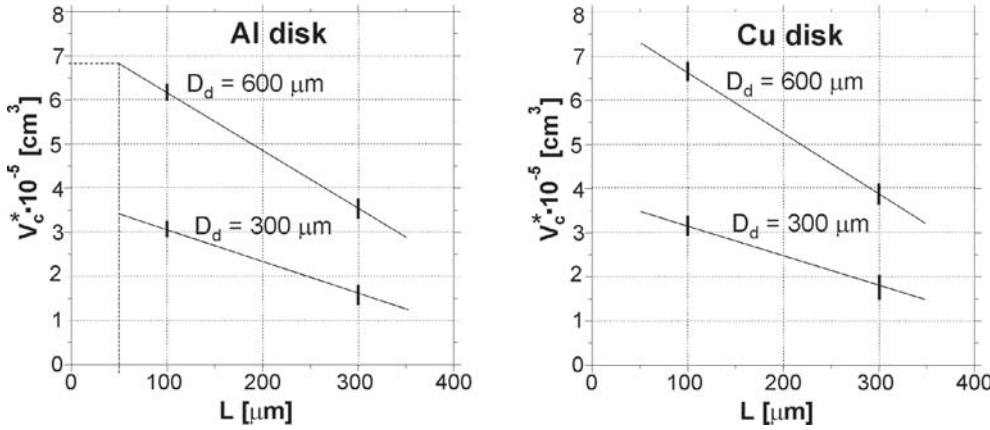


Fig. 6. Average crater volume dependences on the separation distance for the two disk diameters and different disk materials. The vertical lines in the tested points of the crater volumes inform about obtained dispersions of the crater volumes for a few shots.

		$D_d = 300 \mu\text{m}$		$D_d = 600 \mu\text{m}$	
		$L = 100 \mu\text{m}$	$L = 300 \mu\text{m}$	$L = 100 \mu\text{m}$	$L = 300 \mu\text{m}$
Disk material	Al	3.05	1.62	6.16	3.54
	Cu	3.15 (2.90*)	1.81 (1.66*)	6.62 (6.09*)	3.88 (3.57*)

Table 1. The set of average crater volumes in (10^{-5}) cm^3 . The volumes with the star are products of the measured volumes of the craters (in brackets) and the coefficient of 0.92.

($2.97 \times 10^{-3} \text{ g/cm}^2$ for the Al disks and $3.23 \times 10^{-3} \text{ g/cm}^2$ for the Cu ones), the crater volumes produced by the Cu disks should be multiplied by the coefficient of 0.92 to be comparable with those produced by the Al disks.

The average crater volumes corresponding to all investigated cases are presented in Table 1. The values with the star are related to the measured crater volumes produced by the Cu disks multiplied by 0.92. These values are very close to those for the Al disks.

4 Discussion of the experimental results

The experimental results related to the disk produced craters provided plethora of interesting details with respect to the disk acceleration and crater creation processes. In general, there is a well established fact that the solid angle of the plasma emission depends on the plasma source size and grows with decreasing diameter of the plasma emission surface (reaching the half-space for the ideal point plasma source). Therefore, it comes as no surprise that our interferometric measurements confirm beyond any doubts the smaller divergence of the plasma emission resulting from the larger diameter of the plasma source (i.e. the $600 \mu\text{m}$ diameter disk). It is quite likely that the plasma emission diameters in the both cases are very close to the corresponding disk diameters.

This feature could be explained the following way: if the irradiated target is very thin, like the thin foil used in our experiments, the absorbed laser energy will spread from the absorption region also to the surrounding (not irradiated) regions of the target. This lateral transfer of heat causes considerable growth of the ablated target material effective diameter. The energy density accumulated in such thin targets depends on their surface (i.e. diameter). Therefore the greater energy density in the case of the

smaller disk results likely in the bigger plasma density (see Fig. 4).

Summarizing, the above considerations allow to infer that higher thermodynamical state of smaller disks leads to faster run of subsequent hydrodynamical processes inside the disk, such as compression and rarefaction of the disk material.

The main problem of the optimization of the disk parameters concerns the choice of the most suitable disk diameter with respect to the laser spot, laser energy, gap, etc. As it was mentioned earlier, our investigations have shown that the focal spot diameter only a bit smaller than the disk diameter doesn't necessarily assure the most effective utilization of the laser energy. Understanding of this phenomenon became much clearer thanks to the paper [12], where a theoretical two-dimensional model of the plasma plume (produced as a result of the evaporation of the target material irradiated by the laser pulse with constant intensity) in combination with a quasi-one-dimensional model of the shock wave (propagating through the non-vaporized part of the target under the pressure of the plasma plume) are employed. According to this model for the best use of the laser energy in the case of the extended plasma source (i.e. plane expansion geometry) the so called plasma scale length ξ should be smaller compared to the disk radius. Otherwise, some part of the ablative pressure is lost. As the laser beam radius is kept constant, ξ grows with increasing laser energy.

In our experiment the laser energy of 120 J corresponds to $\xi = 230 \mu\text{m}$. This means that in the case of the smaller disks with the diameter of $300 \mu\text{m}$ (i.e. the radius of $150 \mu\text{m}$) a significant part of the ablative pressure couldn't be employed. To make sure that the ablative pressure would be completely used, the diameter of a second set of disks was chosen deliberately twice as large ($600 \mu\text{m}$). The results of our experiments seem to be

proving correctness of this theoretical prediction. In fact, the volume of craters produced by the disks with doubled diameters appears to be twice as large.

To determine the disk mass density influence on the crater creation efficiency the two disk materials with considerable difference of their respective mass densities should be used. Obtained parameters of the craters produced by the disks made of Al and Cu in our experiments allow us to conclude that the craters volume and shape should be similar in cases of different disk materials provided the surface mass densities and diameters of the disks would be the same. Of course, this conclusion concerns only metallic disks with not very great difference of mass densities between them.

This conclusion is very important for our further considerations. If we pay our attention to the craters from the point of different gaps used ($L = 100 \mu\text{m}$ or $300 \mu\text{m}$) we see that for the both disk diameters the crater volumes in case of $L = 100 \mu\text{m}$ are about twice as large as those in case of $L = 300 \mu\text{m}$. Because the crater depth at any given point is determined by the disk surface mass density corresponding to this point one can suppose that the smaller depth of the craters in the case of the gap of $300 \mu\text{m}$ results from the smaller disk surface mass density.

This could be explained the following way: the disk during the laser action is heated due to the thermal conductivity and the shock wave propagation. At the end of the shock wave propagation the disk with a very high internal energy undergoes decompression. The rarefaction wave, which appears and propagates in the compressed disk, has its velocity equal to that of the acoustic one. It is a relatively high velocity, higher than the velocity of the preceding shock wave, the value of which in the case of the Al target was calculated to be on the level of $2 \times 10^6 \text{ cm/s}$ [12]. The fast decompression of the disk leads to the loss of a certain fraction of the disk mass. As this process is taking place during the whole time of the remaining disk flight before the impact, the larger the gap, the lower is the disk surface mass density.

Similar situation can be observed for the craters produced by the disks with different diameters and the same gaps. In the case of larger disk diameters the craters are created deeper. However, the crater diameters for the both disk diameters are only slightly different. Assuming that the total internal energy deposited inside the both disks is the same and taking into account that the larger disk volume is 4 times bigger than that of the smaller one, we come to conclusion that the process of the disk decompression ran much faster in the case of the smaller disk. Thus, at the same instant of the disk flight, in the case of the smaller disk one can expect a greater relative growth of the disk diameter at the simultaneous decrease of the disk surface mass density. Consequences are similar to those observed in the case of the greater gap for the disks with the same diameter.

In these considerations the influence of the ablative pressure action, mentioned above, was omitted. According to our opinion, in the absence of the disk heating, the craters depths for the both disk diameters should differ

much less. However in the case of the smaller disk the crater diameter should be smaller.

The crater profiles presented in the paper demonstrate that most of the craters have a trapezoidal shape which corresponds to the planar shock wave induced by the disks. However, the shapes of the craters produced by the disks with the diameter of $300 \mu\text{m}$ and located at the distance of $300 \mu\text{m}$ are essentially different. Their relatively small diameters suggest disintegration of the outer part of the disks. Since the shape of these craters have a conical form, one can suppose that the disintegration of these disks starts from their edge and moves gradually to their centre. In the case of the larger disks this disintegration has more uniform character.

The crater creation efficiency depends on the disk thickness, too. A proper choice of the disk thickness is very important from the point of view of the efficiency of the disk acceleration. If the disk thickness is too big, the shock wave generated by the ablative pressure is not able to pass through the disk during the laser beam action. In this case the kinetic energy of the disk corresponds to that of the disk material behind the shock wave. In our experiments the shock wave velocity in the Al disks was estimated of the level of $2 \times 10^6 \text{ cm/s}$. The disk material velocity behind the shock wave was expected to be slightly smaller. Therefore, the disk thickness should be chosen in such a way that the shock wave travel time through the disk should be relatively short compared to the laser pulse duration. In such case, after the shock wave passes through the disk, the rest of the laser pulse is employed for the free disk acceleration. In our $11 \mu\text{m}$ thick Al disk the shock wave reaches the rear side of the disk after about 0.5 ns. Because the PALS laser pulse has a Gaussian-like shape with 0.4 ns of FWHM, one can suppose that the shock wave passed through the disk around the laser pulse maximum. Therefore, the second half of the laser pulse could be used for the disk acceleration. Since the velocity of the $11 \mu\text{m}$ thick Al disk with the diameter of $300 \mu\text{m}$ equals to $4.0 \times 10^6 \text{ cm/s}$ (the value measured in our earlier experiments using the same irradiation conditions [16]) which is twice as high than that of the shock wave mentioned above, one can conclude that in these experiments a considerable part of the laser pulse was employed for the disks acceleration. A thinner disk thus might be a better choice from the point of view of its final velocity reached. However, on the other hand, a too thin disk can undergo faster decomposition and, consequently, should be located closer to the massive component of the double target. Simultaneously, such a distance should ensure a possibility for effective disk acceleration.

Following this line of thoughts we came to the conclusion that the proper choice of the distance between the disk and the massive target is very important. In our earlier experiments the maximum velocity of disk or foil was found to be reached after about 2–3 ns [16]. Assuming the constant disk acceleration during that stage the average velocity would be equal to one half of the measured maximum velocities: $4.0 \times 10^6 \text{ cm/s}$ for the $300 \mu\text{m}$ diameter disk and near $3.4 \times 10^6 \text{ cm/s}$ for the $600 \mu\text{m}$ diameter

disk [16] (the second velocity value was measured for a 11 μm thick Al foil). Under these assumptions the distance at which the disk reaches its maximum velocity can be estimated to about 50 μm . Any shorter distance should provide worse results from the point of the created crater volume. Based on the diagrams presented in Figure 6 and assuming that the function of $V_c(L)$ has a linear character, one can come to the conclusion that the maximum possible crater volume (corresponding to $L = 50 \mu\text{m}$) for the disk with the diameter of 600 μm could be close to $7 \times 10^{-5} \text{ cm}^3$. This value is still somewhat smaller compared to that obtained for the direct laser action under the same irradiation conditions (about $8.5 \times 10^{-5} \text{ cm}^3$). This finding leaves an open question if the disk impact method even under the optimal conditions can be at least as (if not more) effective as the direct laser action.

5 Conclusions

The indirect method of laser action exhibits some useful features. By changing the flyer target parameters as well as its location and irradiation it is possible to obtain a wide range of macroparticle velocities and diameters.

However, the processes of acceleration and collision of the disk with the massive target are very complex due to many accompanying physical phenomena. As a result of that determination of the most suitable set of the disk parameters, its time of flight and irradiation conditions from the point of view of the crater creation efficiency represents a very challenging task. All these parameters are mutually interrelated and any change of one of them implies necessity of corresponding changes of the others as well. In spite of that our investigations allowed us to come to some conclusions as follows:

- plasma emission properties, such as plasma stream divergence and electron density distribution, depend strongly on the disk diameter;
- the crater volume and shape should be similar in the case of different disk materials provided that their surface mass densities are the same;
- to use effectively the laser energy the disk diameter should be considerably greater than the focal spot one;
- the important role in the efficiency of the crater creation plays the distance between the disk and the massive target.

Results coming from our optimization attempts aren't so far fully conclusive. To deal with many of the remaining question marks connected with this problem would require to test the parameters under consideration by varying their values over the wide ranges. Nevertheless, our new experience accumulated during these experiments helped us to get a deeper insight into the complexity of this problem.

Finally, we would like to emphasize that the results of these investigations made it possible to explain some doubts connected with the efficiency of the crater creation by the flyer disks. It seems that a proper choice of the disk parameters can allow to reach this efficiency on the level of that for the direct laser action.

References

1. D. Batani, A. Balducci, D. Berenta, A. Bernardinello, *Phys. Rev. B* **61**, 9287 (2000)
2. R. Cauble, D.W. Phillion, T.J. Hoover, N.C. Holmes, J.D. Kilkenny, R.W. Lee, *Phys. Rev. Lett.* **70**, 2102 (1993)
3. K.A. Tanaka, M. Hara, N. Ozaki, Y. Sasatani, S.I. Anisimov, K. Kondo, M. Nakano, K. Nishihara, H. Takenaka, M. Yoshida, K. Mima, *Phys. Plasmas* **7**, 676 (2000)
4. N. Ozaki, Y. Sasatani, K. Kishida, M. Nakano, K. Nagoi, K. Nishihara, T. Norimatsu, K.A. Tanaka, Y. Fujimoto, K. Wakabayashi, S. Hattori, T. Tange, K. Kondo, M. Yoshida, N. Kozu, M. Ishiguchi, H. Takenaka, *J. Appl. Phys.* **89**, 2571 (2001)
5. R. Verker, N. Eliaz, I. Gouzman, S. Eliezer, M. Fraenkel, S. Maman, F. Beckmann, K. Pranzas, E. Grossman, *Acta Mater.* **52**, 5539 (2004)
6. F. Cottet, *Appl. Phys. Lett.* **47**, 678 (1985)
7. R. Fabbro, B. Faral, J. Virmont, H. Pepin, F. Cottet, J.P. Romain, *Laser Part. Beams* **4**, 413 (1986)
8. A. Caruso, V.A. Pais, *Nucl. Fusions* **36**, 745 (1996)
9. M. Murakami, H. Nagatomo, T. Sakaiya, H. Azechi, S. Fujioka, H. Shiraga, M. Nakai, K. Shiramori, H. Saito, S. Obenschain, M. Karasik, J. Gardner, J. Bates, D. Colombant, J. Weaver, Y. Aglitskiy, *Plasma Phys. Control. Fusion* **47**, B815 (2005)
10. K.S. Gus'kov, S.Yu. Gus'kov, *Quant. Electron.* **31**, 305 (2001)
11. A.E. Bolkhovitinov et al., *Phys. Plasma* **30**, 205 (2004)
12. S.Yu. Gus'kov, S. Borodziuk, M. Kalal, A. Kasperczuk, B. Kralikova, E. Krousky, I. Limpouch, K. Masek, P. Pisarczyk, M. Pfeifer, K. Rohlena, J. Skala, J. Ullschmied, *Quant. Electron.* **34**, 989 (2004)
13. J. Limpouch, N.N. Demchenko, S.Yu. Gus'kov, M. Kalal, A. Kasperczuk, V.N. Kondrashov, K. Masek, P. Pisarczyk, T. Pisarczyk, V.B. Rozanov, *Plasma Phys. Control. Fusion* **46**, 1831 (2004)
14. A. Kasperczuk, S. Borodziuk, N.N. Demchenko, S.Yu. Gus'kov, M. Kalal, V.N. Kondrashov, B. Kralikova, E. Krousky, J. Limpouch, K. Masek, M. Pfeifer, P. Pisarczyk, T. Pisarczyk, K. Rohlena, V.B. Rozanov, J. Skala, J. Ullschmied, *31st EPS Conference on Plasma Phys.* London, 2004, ECA, Vol. 28G, p. 5.067 (2004)
15. T. Pisarczyk, S. Borodziuk, N.N. Demchenko, S.Yu. Gus'kov, M. Kalal, A. Kasperczuk, V.N. Kondrashov, J.V. Limpouch, P. Pisarczyk, K. Rohlena, V.B. Rozanov, J. Skala, J. Ullschmied, *28th European Conference on Laser Interaction with Matter*, Roma, 2004, p. 465-469.
16. S. Borodziuk, N.N. Demchenko, S.Yu. Gus'kov, K. Jungwirth, M. Kalal, A. Kasperczuk, V.N. Kondrashov, B. Kralikova, E. Krousky, J. Limpouch, K. Masek, P. Pisarczyk, T. Pisarczyk, M. Pfeifer, K. Rohlena, V.B. Rozanov, J. Skala, J. Ullschmied, *Opt. Applicata* **35**, 241 (2005)
17. K. Jungwirth, A. Cejnarova, L. Juha, B. Kralikova, J. Krasa, E. Krousky, P. Krupickova, L. Laska, K. Masek, A. Prag, O. Renner, K. Rohlena, B. Rus, J. Skala, P. Straka, J. Ullschmied, *Phys. Plasmas* **8**, 2495 (2001)